Current Biology 23, 1579–1584, August 19, 2013 ©2013 Elsevier Ltd All rights reserved http://dx.doi.org/10.1016/j.cub.2013.06.041

Report

MicroRNAs Act as Cofactors in Bicoid-Mediated Translational Repression

Claudia J. Rödel,[1] Anna F. Gilles,[2] and Michalis Averof[1,2,3,*]
[1]Institute of Molecular Biology and Biotechnology (IMBB), Foundation for Research and Technology Hellas (FoRTH), 70013 Heraklio, Crete, Greece
[2]Institut de Génomique Fonctionnelle de Lyon (IGFL), École Normale Supérieure de Lyon, 46 allée d'Italie, 69364 Lyon, France
[3]Centre National de la Recherche Scientifique (CNRS), France

Summary

Noncoding RNAs have recently emerged as important regulators of mRNA translation and turnover [1, 2]. Nevertheless, we largely ignore how their function integrates with protein-mediated translational regulation. We focus on Bicoid, a key patterning molecule in *Drosophila*, which inhibits the translation of *caudal* in the anterior part of the embryo [3, 4]. Previous work showed that Bicoid recruits the cap-binding protein d4EHP on the *caudal* mRNA to repress translation [5]. Here we show that *miR-2* family microRNAs are essential cofactors in the repression of *caudal*. Using an in vivo sensor, we demonstrate that Bicoid acts through a 63 nt response element in the *caudal 3′ UTR* that includes a single *miR-2* target site. Mutating that site abolishes Bicoid-mediated repression, and this effect can be partly reversed by expressing a microRNA with compensatory changes that restore binding to the mutated target. Four predicted Bicoid splice isoforms are capable of *caudal* repression, including two that lack the d4EHP interaction domain; all four isoforms require the microRNA target for repression. The synergy between Bicoid and microRNAs appears to have evolved recently in the context of the drosophilid *caudal BRE*. The discovery that microRNAs play an essential role in Bicoid-mediated translational repression opens up new perspectives on Bicoid's function and evolution.

Results and Discussion

Bicoid (Bcd) is a key regulator that functions as a morphogen to define the anterior-posterior axis of *Drosophila* embryos [6, 7]. It fulfils this role by acting both as a transcriptional activator and as a translational repressor of different target genes in early blastoderm embryos [3, 4, 8–10]. Bicoid evolved recently, within cyclorrhaphan flies, from a homeobox-containing gene of the Hox family [11–14], by acquiring a suite of new properties that include its anterior localization in early embryos, a major change in its DNA binding specificity, and the ability to bind RNA and to regulate translation [15]. Bicoid thus serves as an excellent paradigm for the evolution of gene functions.

The only known translational target of Bicoid is the posterior patterning gene *caudal*, whose maternally transcribed messenger RNAs (mRNAs) are ubiquitously distributed in early embryos [3, 4]. Bicoid-mediated translational repression generates an inverse (posterior) gradient of Caudal (Cad) protein (Figure 1A). Previous work showed that *caudal* repression involves direct binding of the Bicoid homeodomain to the 3′ untranslated region (UTR) of *caudal* mRNA and recruitment of the cap-binding protein d4EHP [3–5, 16, 17]. This mechanism has served as a new paradigm for translational repression via competitive cap binding [18]. Here we report that Bicoid-mediated repression is more complex than previously thought and involves an unsuspected contribution from microRNAs.

In Vivo Sensor for Bicoid-Mediated Translational Repression

To monitor Bicoid's ability to regulate translation in vivo, we established a fluorescent sensor. It consists of a transgene expressing nuclear-localized EGFP followed by the *caudal 3′ UTR*, under the constitutive *tub-α1* promoter (Figure 1B). A control sensor contains the SV40 early polyadenylation sequence instead of the *caudal 3′ UTR*. We inserted both constructs at the same location in the *Drosophila* genome using phiC31-mediated integration (see the Supplemental Experimental Procedures available online). Flies carrying these constructs expressed high levels of EGFP protein in their ovaries, which perdured to embryonic stages. This ubiquitous maternal EGFP prevented us from observing Bicoid-mediated translational repression in early embryos. However, by expressing Bicoid protein uniformly in oocytes and early embryos, using *nanos-GAL4* and a *UAS-Bcd* construct carrying the *fs(1)K10 3′ UTR* instead of the *bicoid 3′ UTR*, we observed that Bicoid exerted a strong repression on the *caudal 3′ UTR* sensor (Figure 1B). The control sensor, carrying the SV40 polyA, was insensitive to Bicoid (Figure 1B). Thus, we developed a sensor that recapitulates Bicoid-mediated repression on the *caudal 3′ UTR* during oogenesis.

Using a modified sensor, expressing an unstable EGFP-Cad fusion protein with the *caudal 3′ UTR*, we were able to detect the graded activity of Bicoid in early embryos (see Figure S1A). However, the weaker and graded fluorescence obtained with that sensor was less reliable for quantitative measurements.

Bicoid Isoforms Lacking the d4EHP-Interaction Domain Are Still Capable of Repression

The five known splice isoforms of *bicoid* are predicted to encode different protein isoforms (http://flybase.org; Figure 1C), but potential functional differences of these isoforms had not been tested. We examined the functional properties of each Bicoid isoform by generating UAS lines for each isoform and expressing them uniformly in the oocyte and early embryo using the *nanos-GAL4* driver (see the Supplemental Experimental Procedures).

The transcriptional capability of each isoform was tested by examining the expression of a known transcriptional target of Bicoid, *hunchback*, in embryos. We found that isoforms D to G are capable of driving ectopic *hunchback* expression, whereas isoform A, which lacks the homeodomain, is not (see Figure S1B). Next we examined the translational capability of each isoform using the *caudal 3′ UTR* sensor described earlier. Isoforms D to G repressed the sensor, whereas isoform A had no effect (Figure 1D). Consistent results were obtained using different *UAS-Bcd* insertions. Repression by isoforms D to G

*Correspondence: michalis.averof@ens-lyon.fr

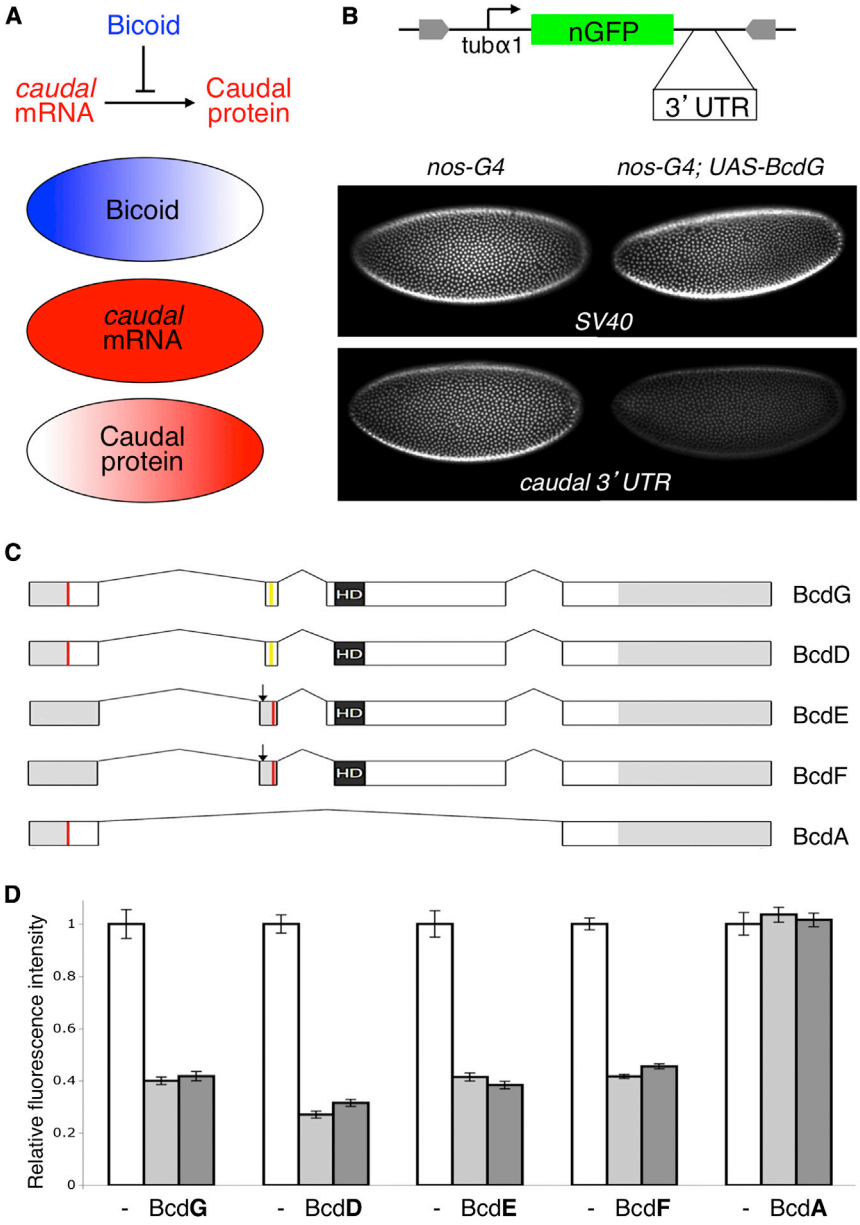

Figure 1. In Vivo Sensor Reveals Translational Regulation by Bcd Isoforms

(A) Schematic representation of Bicoid and Caudal distributions in early *Drosophila* embryos. Maternal *caudal* mRNA is uniformly distributed. The anterior gradient of Bcd represses *caudal* translation, resulting in an opposite gradient of Caudal protein [3, 4].

(B) The in vivo sensor of Bcd-mediated translation consists of a maternally active promoter (*tub-α1*) driving expression of nuclear-localized EGFP followed by 3′ UTR sequences whose activity we are testing. Using the sensor carrying the *SV40 3′ UTR*, we observe high levels of GFP fluorescence in blastoderm embryos, both in the presence and absence of maternally expressed Bcd (*nos-GAL4* versus *nos-GAL4; UAS-BcdG*). In contrast, we observe that Bcd is able to exert a strong repression on the sensor carrying the *caudal 3′ UTR*. Fluorescence images for each sensor were captured using identical settings. The *SV40 3′ UTR* sensor is expressed at higher levels than the *caudal 3′ UTR* sensor, so we used shorter exposure times to image those embryos.

(C) Representation of the five splice isoforms of Bcd (see http://flybase.org). The longest protein isoform is BcdG. Isoforms D and F utilize an alternative splice acceptor in exon 3, generating proteins that lack a short sequence just upstream of the homeodomain (HD). Isoforms E and F utilize an alternative splice acceptor in exon 2, which results in the introduction of a stop codon (arrow) in frame with the first AUG; an alternative in-frame AUG in exon 2 may be used to initiate translation in these mRNAs (AUG start codons marked in red). Isoform A lacks exons 2 and 3, generating a protein that lacks both the homeodomain and the d4EHP-interaction domain. Putative coding sequences are shown in white, 5′ and 3′ UTRs in gray, the d4EHP interaction domain [5] is marked in yellow and the homeodomain (HD) in black.

(D) Assaying translational repression ability of each Bcd isoform using the *caudal 3′ UTR* sensor. Fluorescence was quantified on cycle 11 blastoderm embryos laid by females carrying single insertions of the sensor, *nanos-GAL4* and *UAS-Bcd*; two lines, carrying different insertions of the *UAS-Bcd* transgene, were tested for each isoform (gray bars). The mean fluorescence intensity of each set was quantified in relation to control embryos from females carrying the sensor and *nos-GAL4* (white bars). Note that isoforms E and F, which lack the characterized d4EHP interaction domain, are still capable of robust repression. Error bars represent one SE.

See also Figures S1 and S2.

was also seen with Caudal antibody stainings in early embryos (Figure S1C). Sensor mRNA levels are not significantly affected by the presence of Bicoid isoforms D to G (Figure S2A), suggesting that these isoforms exert their effects primarily by translational repression. These results show that isoforms D to G are all potentially contributing to the transcriptional and translational activities of Bicoid, whereas isoform A is unlikely to do so.

Strikingly, isoforms E and F lack the d4EHP-binding domain, which is thought to be necessary for translational repression via d4EHP recruitment and competitive inhibition at the cap [5]. The fact that these isoforms are equally capable of repressing *caudal* suggests the existence of alternative mechanisms of Bicoid-mediated translational repression.

The *caudal 3′ UTR* Contains a Bicoid-Response Element with a Putative MicroRNA Target Site

To examine how Bicoid exerts its repression, we identified a short fragment of the *caudal 3′ UTR* that can mediate Bicoid-dependent repression in vivo. Previous work had defined a 350 nt Bicoid response element (BRE) [3]. Guided by sequence conservation, we narrowed that activity down to a 63 nt fragment, *BRE(257–319)*, that encompasses nucleotides 257–319 of the *caudal 3′ UTR* (Figure 2). When incorporated into the control sensor construct, this fragment recapitulates Bicoid-dependent repression (Figure 2E). Bicoid does not significantly reduce *BRE(257–319)* sensor mRNA levels (Figure S2B), suggesting that the effect is largely due to translational repression.

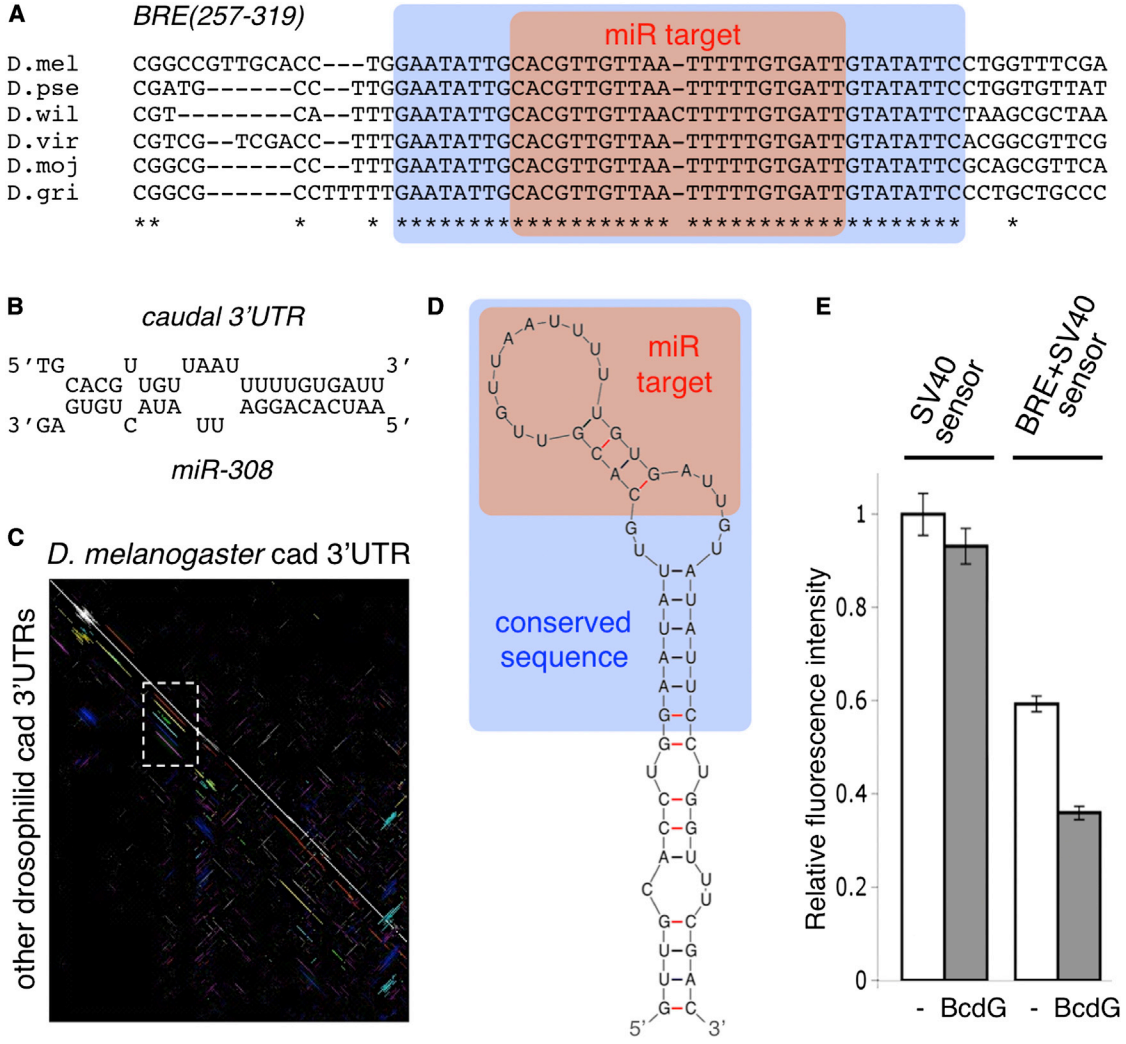

Figure 2. The Bicoid Response Element in the *Caudal 3′ UTR* Contains a Putative MicroRNA Binding Site

(A) Sequence alignment of *BRE(257–319)* among drosophilid species. The conserved sequence and putative microRNA target site are highlighted in blue and red, respectively.

(B) Predicted interaction of putative microRNA target site in the *caudal 3′ UTR* with *Drosophila miR-308*; similar interactions are predicted with other microRNAs that share the *miR-2* seed sequence (*miR-2*, *miR-6*, *miR-11*, *miR-13*, and *miR-308* [19, 20]).

(C) Dot plot of *Drosophila melanogaster caudal 3′ UTR* sequence compared to the homologous 3′ UTRs of other drosophilid species. Different pairwise comparisons are shown in separate colors. The only region where all drosophilid sequences show significant conservation is indicated in the box.

(D) Putative RNA secondary structure of *BRE(257–319)*; the conserved portion of the sequence and the putative microRNA target site are highlighted.

(E) *BRE(257–319)* is sufficient to mediate Bcd-dependent repression in vivo. We compare the activities of a control sensor, carrying the *SV40 3′ UTR*, and a sensor carrying *BRE(257–319)* just upstream of the *SV40 3′ UTR*. Fluorescence was quantified in cycle 11 blastoderm embryos laid by females carrying single insertions of each sensor and *nanos-GAL4*, in the presence or absence of *UAS-BcdG* (white and gray bars, respectively). The mean fluorescence intensity of each set was quantified in relation to the control sensor in the absence of Bcd. The presence of *BRE(257–319)* confers Bcd sensitivity to the *SV40 3′ UTR*. Lower overall fluorescence levels in the *BRE(257–319)* sensor could be mediated by the microRNA target site. Error bars represent one SE. We note that the *BRE(257–319)* sensor is expressed at much higher levels than the *caudal 3′ UTR* sensor, in the absence of Bicoid, suggesting that additional elements outside of *BRE(257–319)* contribute to *caudal mRNA* repression independently of Bicoid.

See also Figures S2 and S3.

As we describe below, certain mutations within *BRE(257–319)* abolish responsiveness to Bicoid. Thus, elements contained within *BRE(257–319)* are both necessary and sufficient to mediate responsiveness to Bicoid.

BRE(257–319) displays a number of interesting features. First, within the *caudal 3′ UTR*, it is the region with the highest degree of sequence conservation among drosophilids (Figures 2A and 2C). Second, RNA secondary structure predictions suggest that the fragment may fold into a stable hairpin structure (Figure 2D). Third, the distal part of that hairpin harbors a putative target site for microRNAs of the *miR-2* family, including microRNAs *miR-2*, *miR-6*, *miR-11*, *miR-13*, and *miR-308*, which share the same seed sequence (Figure 2B). The putative microRNA target lies at the center of the conserved region. The presence of a conserved microRNA target site within the Bicoid-responsive element suggests that the translational regulation of *caudal* could involve an interaction between Bicoid and microRNAs.

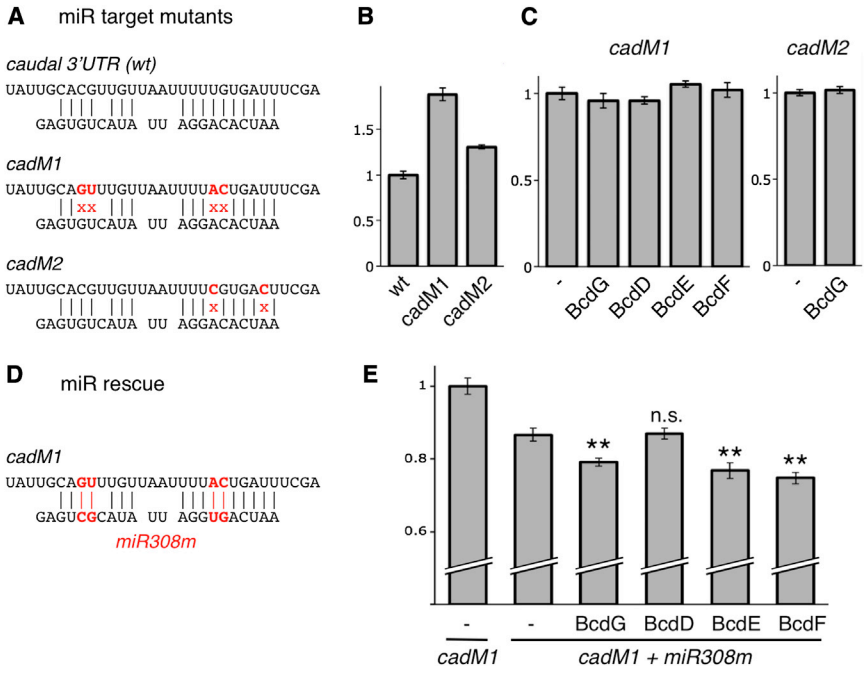

Figure 3. The MicroRNA Target Site in *BRE(257–319)* Is Essential for Bcd-Mediated Repression

(A) To test the role of microRNA binding, we generated two sets of mutations in the *caudal 3′ UTR*, named *cadM1* and *cadM2*, which are predicted to completely disrupt binding of *miR2* family microRNAs. The mutations (highlighted in red) disrupt binding at the microRNA seed sequence [21, 22] but preserve the secondary structure of the 3′ UTR (shown in Figure 2D).

(B) The fluorescence intensity of the *cadM1* and *cadM2 in vivo* sensors was quantified in cycle 11 blastoderm embryos, relative to the intensity of the wild-type *caudal 3′ UTR* sensor ("wt"), in the absence of Bcd. Both mutant sensors displayed significantly higher fluorescence levels than the wild-type.

(C) The fluorescence intensity of the *cadM1* and *cadM2* sensors was not affected by the expression of Bcd (embryos laid by *nos-GAL4*; *UAS-Bcd* females).

(D) To rigorously test the requirement of microRNA binding for Bcd-mediated repression, we asked whether sensitivity to Bicoid can be recovered by providing a mutated microRNA (*miR308m*) that restores binding to *cadM1*.

(E) The fluorescence intensity of the *cadM1* sensor is reduced in the presence of *miR308m*, and sensitivity to Bcd is partially restored. The strength of Bcd-mediated repression is limited, but highly significant with Bcd isoforms G, E, and F. We do not detect an effect with Bcd isoform D, which may point to additional isoform-specific requirements.

All error bars represent one SE (two asterisks indicate 99% statistical confidence; n.s. indicates no statistical significant difference, using a t test).

Mutations in the MicroRNA Target Site Abolish Bicoid-Mediated Repression

To directly test whether the putative microRNA target site is necessary for Bicoid-mediated repression, we generated two sets of mutations (*cadM1* and *cadM2*) that disrupt microRNA binding while preserving the putative secondary structure of the *caudal 3′ UTR* (Figure 3A). These mutations were introduced into our sensor constructs in the context of the entire *caudal 3′ UTR* and were tested in vivo, in the presence or absence of Bicoid.

In the absence of Bicoid, both mutant sensors gave higher readings than the unmutated *caudal 3′ UTR* sensor (Figure 3B), consistent with the expected repressive effect of microRNA binding. Remarkably, adding Bicoid produced no significant change in expression levels of either *cadM1* or *cadM2* (Figure 3C); all the Bicoid isoforms tested (isoforms D to G) were incapable of repression. These results show that the predicted microRNA target site contains essential elements for Bicoid-mediated repression.

Providing a MicroRNA with Compensatory Changes Restores Bicoid-Mediated Repression

The mutant sensor results are consistent with the idea that microRNAs could be involved in Bicoid-mediated repression. This is plausible, as *miR-2* family microRNAs are expressed during oogenesis and deposited in the early embryo [19, 23]. However, an alternative explanation could be that the same point mutations inadvertently disrupt Bicoid binding in a microRNA-independent manner. To address this issue, we asked whether Bicoid responsiveness in a mutant sensor could be rescued by providing a microRNA carrying compensatory changes that restore binding to the sensor. Such a rescue would demonstrate that microRNAs have a direct role in Bcd-mediated repression.

To conduct this experiment, we took the precursor hairpin for a *miR-2* family member, *miR-308*, and introduced point mutations that restore binding to the *cadM1* sensor (Figure 3D). We also introduced mutations to preserve the secondary structure of the precursor hairpin, in order to allow normal processing of the microRNA [24, 25]. We placed this mutant microRNA, called *miR-308m*, under the constitutive *tub-α1* promoter and inserted it into the *Drosophila* genome, on the same chromosome as *cadM1* (see the Supplemental Experimental Procedures).

The presence of *mir-308m* lowered the expression of the mutant sensor (Figure 3E), partially restoring the levels that we observe with the unmutated *caudal 3′ UTR*. This result suggests that *mir-308m* interacts with *cadM1* in vivo. The repressive effect of *mir-308m* is lower than that of endogenous microRNAs on the wild-type *caudal 3′ UTR* (compare first two columns on Figure 3B with Figure 3E), which could be due to lower expression or inefficient processing of *miR-308m*, or due to lower efficiency of the microRNA-target interaction.

Adding Bicoid further repressed *cadM1* expression in the presence of *mir-308m* (Figure 3E), demonstrating that by restoring the microRNA-target interaction we can partially rescue Bicoid-dependent repression. The extent of Bicoid repression is small but reproducible for Bicoid isoforms G, E, and F (compare with Figure 1D). This result demonstrates that microRNA binding to the *caudal 3′ UTR* has a direct role in Bicoid-dependent repression. The fact that the restoration of Bcd repression is partial may reflect a problem in the biogenesis of the mutant microRNA, or effects of the *cadM1* mutation that are independent of microRNA binding (e.g., unanticipated effects on secondary structure, effects on recruitment of other cofactors).

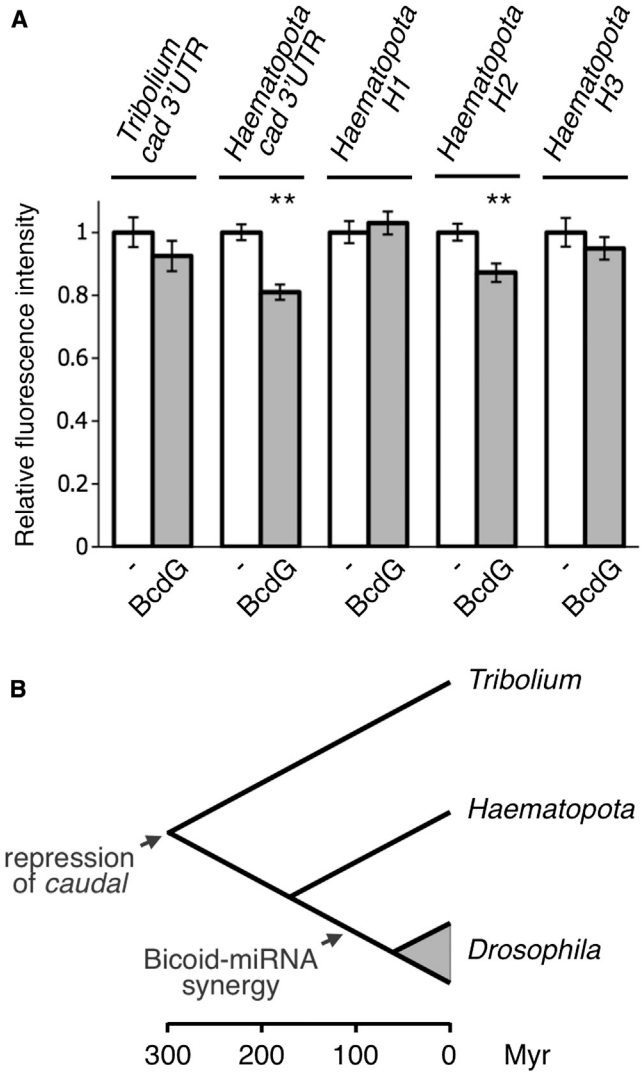

Figure 4. Evolution of Synergy between MicroRNAs and Bcd

(A) Sensors carrying the *Tribolium castaneum* and *Haematopota caudal 3′ UTRs* were assayed for their ability to mediate Bcd-dependent repression. The *Tribolium caudal 3′ UTR* sensor showed no significant difference in the presence or absence of Bcd. In contrast, the *Haematopota caudal 3′ UTR* sensor was significantly repressed by Bcd. To dissect the Bcd-responsive element in *Haematopota caudal 3′ UTR*, we subdivided that sequence into three fragments (*H1*, *H2*, and *H3*) predicted to form distinct stem-loop structures. Sensor constructs show that only one of these fragments, the 42 nt long *H2*, can mediate Bcd-dependent repression. Error bars represent one SE; two asterisks indicate 99% statistical confidence using a t test.

(B) Previous studies have indicated that translational repression of maternal *caudal* mRNA is likely to be an ancient feature that predates the evolution of Bicoid [26, 27]. Although *caudal mRNAs* from *Tribolium*, *Haematopota*, and *Drosophila* may share some *cis*-regulatory signals that can mediate repression by Bcd ([26] and present work), our results suggest that the synergy between microRNAs and Bcd probably arose after the divergence of these species, concomitant with the functional specialization of Bcd in cyclorrhaphan flies [11–15].

See also Figure S4.

MicroRNA-Bicoid Synergy Evolved Recently and Is Context Specific

Translational repression of *caudal* at the anterior pole of the embryo may be an ancient feature that predates the evolution of Bicoid: *caudal* appears to be translationally repressed in the beetle *Tribolium castaneum*, which does not possess a distinct Bicoid homolog [26, 27]. Strikingly, Wolff et al. showed that *Tribolium caudal* mRNA could be repressed in a Bicoid-dependent manner when expressed in *Drosophila* embryos [26], suggesting that Bicoid recognizes the same *cis*-regulatory signal on *caudal* mRNA as the ancestral (Bicoid-independent) mechanism of repression. Could the microRNA target site represent that ancestral conserved signal?

To address this question, we examined the functional properties of *caudal 3′ UTRs* from the beetle *Tribolium castaneum* and the noncyclorrhaphan dipteran *Haematopota pluvialis*, two insects that do not possess Bicoid [11, 13]. A sensor carrying the entire *Tribolium caudal 3′ UTR* showed no significant Bcd-dependent repression in *Drosophila* (Figure 4A), suggesting that the result of Wolff et al. is not mediated through the 3′ UTR. However, we found that a sensor carrying the *Haematopota caudal 3′ UTR* sequence is able to mediate a moderate Bicoid-dependent repression in *Drosophila* (Figure 4A). We mapped this activity to a 42 nt fragment of the *3′ UTR*, that we name *H2*, which is sufficient for Bicoid-dependent repression (Figure 4A). *H2* is predicted to form a hairpin structure and it is capable of weakly binding Bicoid in a gel shift assay in vitro (see Figure S4). Importantly, *H2* lacks any predicted microRNA target sites (including targets for *Drosophila* microRNAs), which suggests that Bicoid acts on this fragment in the absence of microRNA binding.

Thus, we find no evidence to suggest that the role of microRNAs in anterior *caudal* repression predates the evolution of Bicoid (Figure 4B). The synergy of Bicoid with microRNAs appears to have evolved in the context of a specific *caudal BRE* and may be absent outside of the cyclorrhaphan fly lineage.

Conclusions

Our results show that Bicoid cooperates with microRNAs to repress *Drosophila caudal* mRNA. The interaction occurs within a 63 nt region of the *caudal 3′ UTR* and is essential for repression of that specific target. However, microRNAs do not appear to be necessary for Bicoid repression on all targets (see results on the *Haematopota 3′ UTR*), which suggests that the target mRNA plays an important role in determining which components are involved in the repression. Target mRNAs with different sequence or structural motifs may assemble different repressive complexes, involving different sets of proteins and regulatory RNAs.

Bicoid and microRNAs could cooperate in a number of different ways to achieve *caudal* repression. One possible mechanism could involve cooperative binding of Bicoid and microRNA/RISC complexes on the BRE. Although previous work indicated that Bicoid can bind specifically to the *caudal 3′ UTR* in vitro [4, 16, 17], our gel shift experiments suggest that this interaction is weak and not highly specific (see Figure S3). Cooperative binding of microRNAs and Bicoid could enhance the strength and the specificity of this interaction. Bicoid and microRNAs might also cooperate in establishing a translational repression complex that involves several components, including d4EHP and Ago [5, 28]. Thus, the synergy between Bicoid and microRNAs may occur at the level of both mRNA binding and translational repression.

These results point to a previously unappreciated level of complexity in *caudal* repression, involving both proteins and microRNAs, echoing some recent findings in other systems [2, 29, 30]. Bicoid remains the factor that provides the spatial specificity in *caudal* repression, which serves to transmit

positional information in the developing embryo. However, the synergy with microRNAs provides an additional layer of regulation and opportunities for regulatory evolution.

Supplemental Information

Supplemental Information includes Supplemental Experimental Procedures and four figures and can be found with this article online at http://dx.doi.org/10.1016/j.cub.2013.06.041.

Acknowledgments

We thank Urs Schmidt-Ott, Steve Cohen, Gary Struhl, and Pernille Rorth for reagents; Vassilis Paspaliaris, Elpiniki Kalogeropoulou, and Yiannis Livaradas for help with constructs and transgenic lines; Urs-Schmidt-Ott, Jan-Michael Kugler, Steve Cohen, Alexandros Kiupakis, Ernst Wimmer, Gregor Bucher, Fulvia Bono, Kriton Kalantidis, Jordi Casanova, and Maura Strigini for advice and critical comments on the manuscript. This work was supported by the Marie Curie programme "FAMED" (FP6, European Union) and by a scholarship from the Ministry of Education (Greece).

Received: December 21, 2012
Revised: May 14, 2013
Accepted: June 17, 2013
Published: August 1, 2013

References

1. Siomi, H., and Siomi, M.C. (2009). On the road to reading the RNA-interference code. Nature *457*, 396–404.
2. Pasquinelli, A.E. (2012). MicroRNAs and their targets: recognition, regulation and an emerging reciprocal relationship. Nature Rev. Genet. *13*, 271–282.
3. Dubnau, J., and Struhl, G. (1996). RNA recognition and translational regulation by a homeodomain protein. Nature *379*, 694–699.
4. Rivera-Pomar, R., Niessing, D., Schmidt-Ott, U., Gehring, W.J., and Jäckle, H. (1996). RNA binding and translational suppression by bicoid. Nature *379*, 746–749.
5. Cho, P.F., Poulin, F., Cho-Park, Y.A., Cho-Park, I.B., Chicoine, J.D., Lasko, P., and Sonenberg, N. (2005). A new paradigm for translational control: inhibition via 5′-3′ mRNA tethering by Bicoid and the eIF4E cognate 4EHP. Cell *121*, 411–423.
6. Frohnhofer, H.G., and Nusslein-Volhard, C. (1986). Organization of anterior pattern in the Drosophila embryo by the maternal gene bicoid. Nature *324*, 120–125.
7. Driever, W., and Nüsslein-Volhard, C. (1988). The bicoid protein determines position in the Drosophila embryo in a concentration-dependent manner. Cell *54*, 95–104.
8. Driever, W., and Nüsslein-Volhard, C. (1989). The bicoid protein is a positive regulator of hunchback transcription in the early Drosophila embryo. Nature *337*, 138–143.
9. Hanes, S.D., and Brent, R. (1989). DNA specificity of the bicoid activator protein is determined by homeodomain recognition helix residue 9. Cell *57*, 1275–1283.
10. Struhl, G., Struhl, K., and Macdonald, P.M. (1989). The gradient morphogen bicoid is a concentration-dependent transcriptional activator. Cell *57*, 1259–1273.
11. Stauber, M., Jäckle, H., and Schmidt-Ott, U. (1999). The anterior determinant bicoid of Drosophila is a derived Hox class 3 gene. Proc. Natl. Acad. Sci. USA *96*, 3786–3789.
12. Stauber, M., Taubert, H., and Schmidt-Ott, U. (2000). Function of bicoid and hunchback homologs in the basal cyclorrhaphan fly Megaselia (Phoridae). Proc. Natl. Acad. Sci. USA *97*, 10844–10849.
13. Stauber, M., Prell, A., and Schmidt-Ott, U. (2002). A single Hox3 gene with composite bicoid and zerknullt expression characteristics in non-Cyclorrhaphan flies. Proc. Natl. Acad. Sci. USA *99*, 274–279.
14. Lemke, S., Busch, S.E., Antonopoulos, D.A., Meyer, F., Domanus, M.H., and Schmidt-Ott, U. (2010). Maternal activation of gap genes in the hover fly Episyrphus. Development *137*, 1709–1719.
15. McGregor, A.P. (2005). How to get ahead: the origin, evolution and function of bicoid. Bioessays *27*, 904–913.
16. Chan, S.K., and Struhl, G. (1997). Sequence-specific RNA binding by bicoid. Nature *388*, 634.
17. Niessing, D., Driever, W., Sprenger, F., Taubert, H., Jäckle, H., and Rivera-Pomar, R. (2000). Homeodomain position 54 specifies transcriptional versus translational control by Bicoid. Mol. Cell *5*, 395–401.
18. Kong, J., and Lasko, P. (2012). Translational control in cellular and developmental processes. Nat. Rev. Genet. *13*, 383–394.
19. Ruby, J.G., Stark, A., Johnston, W.K., Kellis, M., Bartel, D.P., and Lai, E.C. (2007). Evolution, biogenesis, expression, and target predictions of a substantially expanded set of Drosophila microRNAs. Genome Res. *17*, 1850–1864.
20. Stark, A., Brennecke, J., Russell, R.B., and Cohen, S.M. (2003). Identification of Drosophila MicroRNA targets. PLoS Biol. *1*, E60.
21. Brennecke, J., Stark, A., Russell, R.B., and Cohen, S.M. (2005). Principles of microRNA-target recognition. PLoS Biol. *3*, e85.
22. Bartel, D.P. (2009). MicroRNAs: target recognition and regulatory functions. Cell *136*, 215–233.
23. Votruba, S.M. (2009). microRNAs in the Drosophila Egg and Early Embryo. Master's thesis, University of Toronto.
24. Czech, B., Zhou, R., Erlich, Y., Brennecke, J., Binari, R., Villalta, C., Gordon, A., Perrimon, N., and Hannon, G.J. (2009). Hierarchical rules for Argonaute loading in Drosophila. Mol. Cell *36*, 445–456.
25. Okamura, K., Liu, N., and Lai, E.C. (2009). Distinct mechanisms for microRNA strand selection by Drosophila Argonautes. Mol. Cell *36*, 431–444.
26. Wolff, C., Schröder, R., Schulz, C., Tautz, D., and Klingler, M. (1998). Regulation of the Tribolium homologues of caudal and hunchback in Drosophila: evidence for maternal gradient systems in a short germ embryo. Development *125*, 3645–3654.
27. Schoppmeier, M., Fischer, S., Schmitt-Engel, C., Löhr, U., and Klingler, M. (2009). An ancient anterior patterning system promotes caudal repression and head formation in ecdysozoa. Curr. Biol. *19*, 1811–1815.
28. Singh, N., Morlock, H., and Hanes, S.D. (2011). The Bin3 RNA methyltransferase is required for repression of caudal translation in the Drosophila embryo. Dev. Biol. *352*, 104–115.
29. Kim, H.H., Kuwano, Y., Srikantan, S., Lee, E.K., Martindale, J.L., and Gorospe, M. (2009). HuR recruits let-7/RISC to repress c-Myc expression. Genes Dev. *23*, 1743–1748.
30. Desnoyers, G., and Massé, E. (2012). Noncanonical repression of translation initiation through small RNA recruitment of the RNA chaperone Hfq. Genes Dev. *26*, 726–739.

Current Biology, Volume *23*

Supplemental Information

MicroRNAs Act as Cofactors in Bicoid-Mediated Translational Repression

Claudia J. Rödel, Anna F. Gilles, and Michalis Averof

Supplemental Data

Supplemental Experimental Procedures

Supplemental References

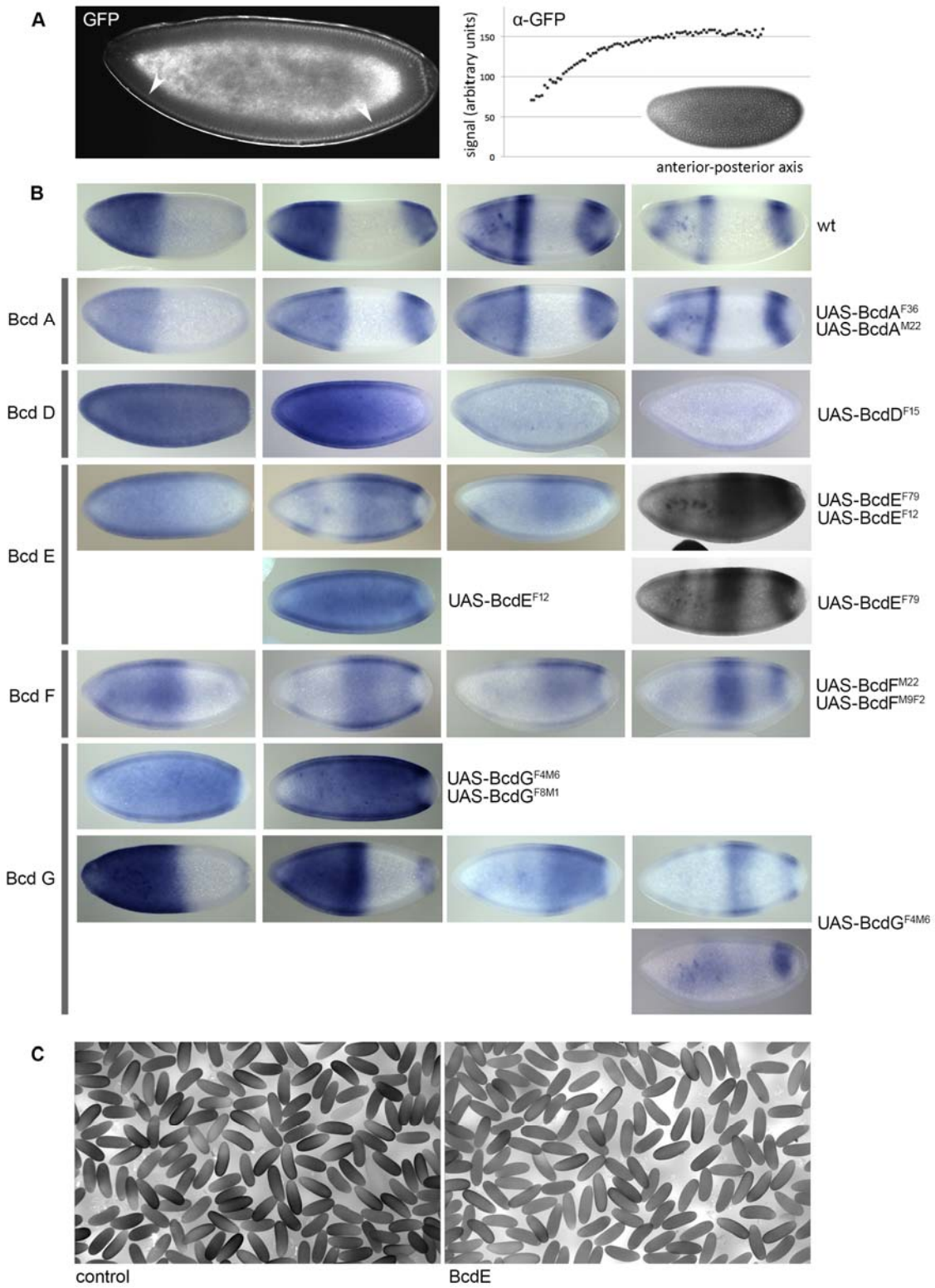

Figure S1. Transcriptional and translational capability of Bicoid isoforms, Related to Figure 1

(A) *In vivo* sensor expressing d2EGFP-Cad fusion protein reveals translational regulation by the endogenous Bicoid gradient. *d2EGFP-Cad* mRNA is expressed maternally and distributed

ubiquitously in early blastoderm embryos (confirmed by *in situ* hybridization, data not shown). The d2EGFP-Cad protein is more unstable than the EGFP protein expressed by the other sensors (weaker overall levels of fluorescence) and therefore less maternally-generated protein perdures in early embryos; this allows us to visualize the new d2EGFP-Cad produced in the early embryos in the presence of the Bcd gradient. The d2EGFP-Cad distribution was visualized in blastoderm embryos by fluorescence (left panel: optical section, nuclear EGFP indicated by white arrowheads) or by staining using an antibody for EGFP (right panel: surface view, with a plot of signal intensity along the anterior-posterior axis). Embryos are shown with anterior to the left.

(B) The expression of *hunchback*, a transcriptional target of Bicoid [S1], was used to assess the transcriptional capability of each Bicoid isoform. *In situ* hybridization with an antisense probe for *hunchback* was carried out in blastoderm embryos laid by wild-type mothers (first row), or by mothers carrying *nanos-GAL4* and *UAS-Bcd* expressing each isoform of Bicoid ectopically (uniformly) in oocytes and early embryos (subsequent rows). The first column shows early zygotic expression near the time of cellularization, the second, third and fourth columns show later stages. Representative expression patterns are shown for independent *UAS-Bcd* transgenic lines (indicated on the right). Shifts in *hunchback* expression are seen in response to isoforms D to G, but not in response to isoform A (expression patterns should be interpreted in the light of results in [S2]). These observations suggest that Bcd isoform A is transcriptionally inactive, while Bcd isoforms D to G show an overlapping range of transcriptional activity. Embryos are shown with anterior to the left.

(C) Staining with an antibody for Caudal in control embryos (laid by *nanos-GAL4* females) and in embryos expressing BcdE (laid by *UAS-BcdE; nanos-GAL4* females), showing that BcdE represses endogenous Caudal expression. The two stainings were performed in parallel, under identical conditions. The same effect was observed with Bcd isoforms D, F and G, but not with Bcd isoform A.

Consistent with these transcriptional and translational effects, embryos uniformly expressing Bicoid isoform A were viable, whereas those expressing isoforms D to G were not.

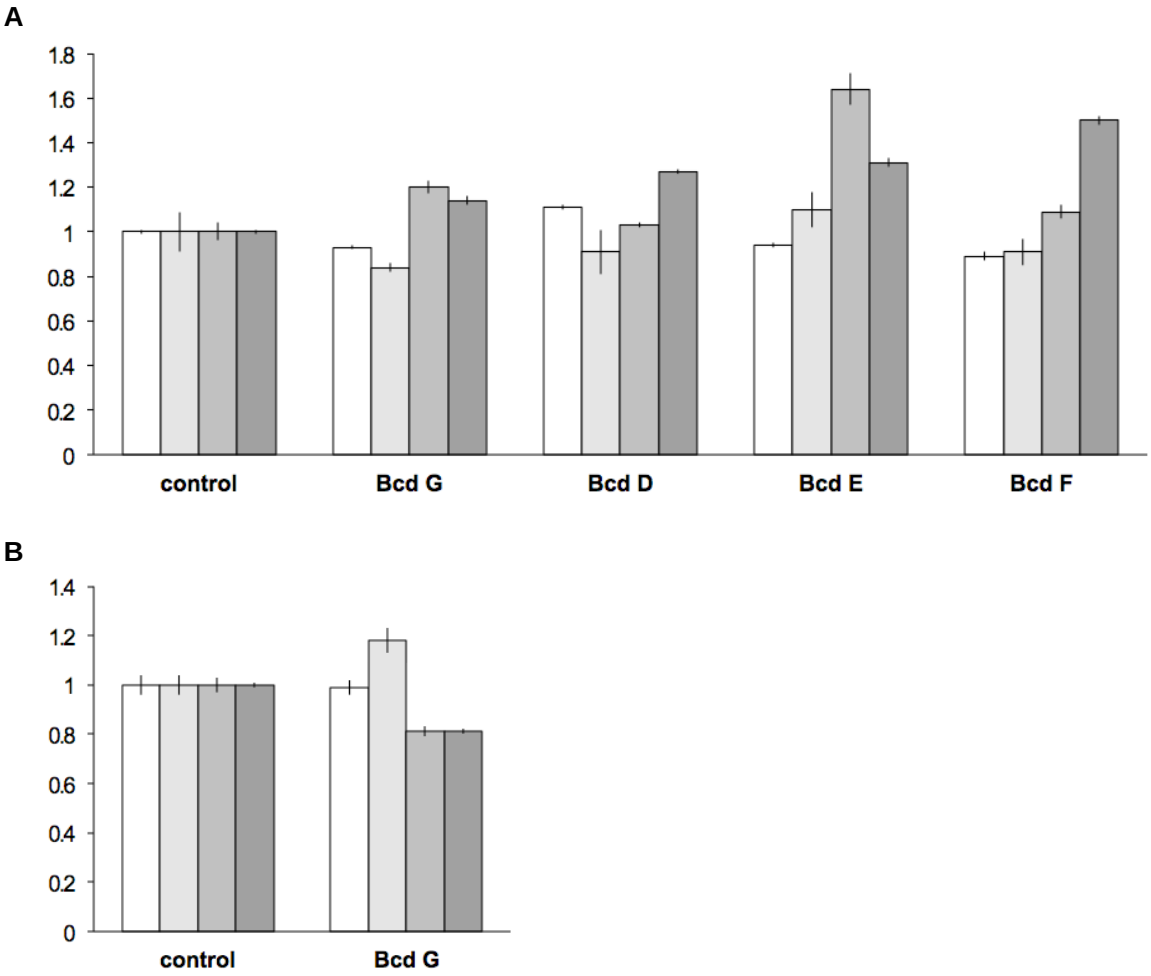

Figure S2. Quantification of sensor mRNA levels by real-time PCR, Related to Figures 1 and 2

(A) Quantification of *caudal 3'UTR* sensor mRNA in ovaries and early embryos expressing individual isoforms of Bcd (mothers carrying a single copy of the sensor, *nanos-GAL4* and *UAS-Bcd*), relative to controls (mothers carrying a single copy of the sensor and *nanos-GAL4*).
(B) Quantification of *BRE(257-319)* sensor mRNA in ovaries and early embryos expressing Bcd isoform G, relative to controls.
For each genotype, measurements were made on two independent ovary samples (first two columns) and two independent embryo collections (third and fourth column). The levels of sensor mRNA were normalized against the levels of *tubulin* $\alpha 1$ mRNA. Error bars represent the standard error of technical replicates.

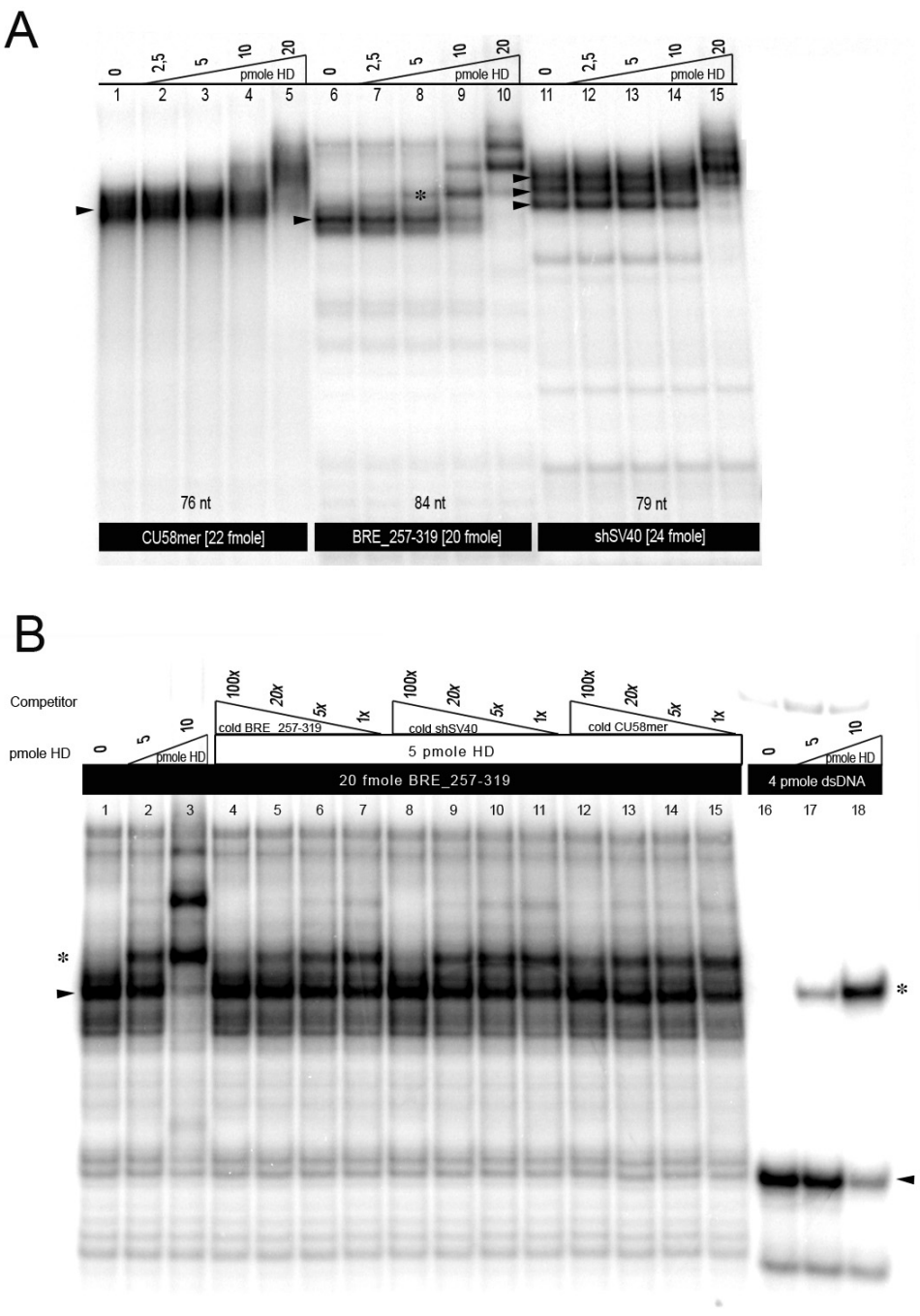

Figure S3. *In vitro* binding specificity of the Bicoid homeodomain, Related to Figure 2
(A) Native electrophoretic mobility shift assay of purified Bicoid homeodomain on three ^{32}P-labelled RNAs. At high concentrations (20 pmole/10µl binding reaction; lanes 5, 10 and 15) the Bicoid homeodomain binds to all three RNAs, including *BRE(257-319)*, a 79-nucleotide RNA containing part of the *SV40 3'UTR* (*shSV40*) and a 58-nucleotide RNA that lacks secondary structure, consisting of a random sequence of C and U (*CU58mer*). At lower concentrations (5-10 pmole/10µl binding reaction) the Bicoid homeodomain binds to *BRE(257-319)* (asterisk, lanes 8-9), but not to *CU58mer* (lanes 3-4) or *shSV40* (lanes 13-14).
(B) Competition experiments testing the stability and specificity of RNA binding of the Bicoid homeodomain. Binding to *BRE(257-319)* could be competed only by adding a large excess of

unlabeled (cold) *BRE(257-319)* RNA (lanes 4-7). *shSV40* was also effective in competing with *BRE(257-319)* binding, but with lower efficiency (lanes 8-11). *CU58mer* had almost no effect on *BRE(257-319)* binding (lanes 12-15). Binding of the Bicoid homeodomain to a DNA fragment that carries a Bcd binding site (*dsDNA*; [S3]) was used as a positive control (lanes 16-18).
Mobility shifts are indicated by an asterisk. Arrowheads indicate the major bands corresponding to the free probe, observed in the lanes where Bcd is absent; multiple bands may be due to alternative RNA secondary structures.

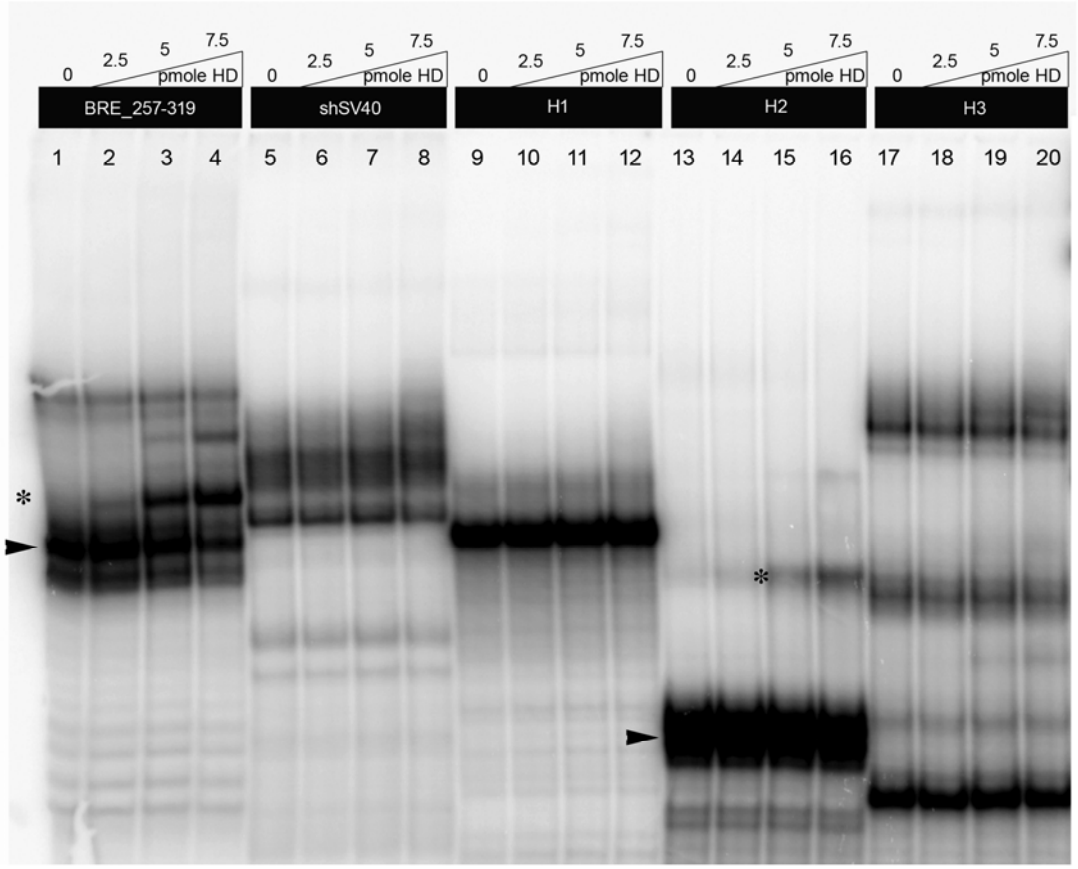

Figure S4. *In vitro* binding of the Bicoid homeodomain to the *Haematopota caudal 3'UTR*, Related to Figure 4

Native electrophoretic mobility shift assay of purified Bicoid homeodomain on ^{32}P-labelled RNAs of *H1, H2* and *H3* ^{32}P-labelled RNA probes, compared to *BRE(257-319)* and *shSV40*. The Bicoid homeodomain binds to *H2*, but not to *H1* or *H3*. The bands corresponding free probe (arrowheads) and mobility shifts (asterisk) are indicated for *BRE(257-319)* and *H2*.

Supplemental Experimental Procedures

Sensor constructs

The sensor constructs were generated in *piB-TdnGFP*, a derivative of *piB-GFP* [S4] which contains the tubulin α1 promoter and the d2EGFP coding sequence (Clontech) fused to the 6xMyc tag and a nuclear localization signal, followed by unique AscI and MluI sites for the cloning of 3'UTR fragments (sequence available on request). The sensor construct is flanked by two inverted *attB* sites.

The *caudal 3'UTRs* of *Drosophila melanogaster* (nucleotides 1-863, numbering from the first nucleotide after the stop codon; GenBank accession NM_057606.5), *Tribolium castaneum* (nucleotides 1-446; GenBank accession NM_001039409) and *Haematopota pluvialis* (nucleotides 1-126; GenBank accession EU295454, [S5]) were amplified by PCR using primer pairs 5'-CGGGATCCATGTGACACGACCATTCC-3' and 5'-TTGGCGCCGTGAA CGTTAACCCTTATTAACC-3', 5'-TTGAATTCTTCCCTCACAACTCATATGACCG-3' and 5'-TGGCGCGCCCAAAATAAAATCATTTATTCTTCAC-3', and 5'-CGGAATTCTGACCACATT AAACGCAT-3' and 5'- AGGCGCGCCCTAAGTAATTTAAGTATAATTA-3', respectively, and cloned into the AscI site of *piB-TdnGFP*. The SV40 3'UTR, taken from pJB26 [S6], was cloned into the MluI site of *piB-TdnGFP*. Fragments of the *Drosophila* and *Haematopota caudal* 3'UTRs were generated by PCR using the following primers: 5'-GTAATACGACTCACTATA GGGCGAATTGGAGCTCGGCCGTTGCACCTGG-3' and 5'- GCGAATTCGAAACCAGGAA TATACAATCAC-3' for *BRE(257-319)*; 5'-GTAATACGACTCACTATAGGGCGAATGACCACA TTAAACGCATTTG-3' and 5'-gctctagaGGCATAACATGGTGACAT-3' for *H1*; 5'- GTAATACG ACTCACTATAGGGCGAATATGCCTATGATCGGTTTTAC-3' and 5'- TGGCGCGCCCATGA TCAGATCAACATCAG-3' for *H2*; 5'-GTAATACGACTCACTATAGGGCGAATTTGAATTAA TTTTAATTATAC-3' and 5'-AGGCGCGCCCTAAGTAATTTAAGTATAATTA-3' for *H3*. These fragments were cloned into AscI site of the SV40 sensor to provide a polyadenylation signal. Forward primers also include the T7 promoter sequence, which was used to generate RNA probes for gel shift experiments (see below).

cadM1 and *cadM2* mutations were introduced by PCR on a *caudal* 3'UTR template, using the overlapping primers 5'-TAACAAACTGCAATATTCCAGGTGCAACGGCCGCCAA GTCCTCCATTCG–3' and 5'-ATTTTACTGATTGTATATTCCTGGTTTCGACACGCGCCAGAG TCCTCACAGC–3' for *cadM1*, and back-to-back primers 5'-GACTGTATATTCCTGGTTTCGA CACG-3' and 5'- ACGAAAATTAACAACGTGCAATATTCCAGG-3' for *cadM2*. The *cadM1* and *cadM2* mutant 3'UTRs were confirmed by sequencing and cloned into the AscI site of *piB-TdnGFP*.

The *d2EGFP-Cad* sensor combines the *hunchback* maternal promoter *(hbP1)*, the *d2EGFP* coding sequence fused to the *caudal* coding sequence, and the *caudal 3' UTR*. The *hbP1* promoter was subcloned from pChbP1ΔXbaI [S7] into the SphI and KpnI sites of *piB-TdnGFP*, replacing the *tubulin α1* promoter. The *caudal* coding sequence was amplified by PCR using primers 5'-CCCTAGGAATGGTTTCGCACTACTACAAC-3' and 5'-CGGCGCGCC TCACATCGAGAGCGTGC-3' (incorporating AvrII and AscI sites, respectively) and cloned downstream of *d2EGFP*, fusing the *d2EGFP* and *caudal* open reading frames and removing the 6xMyc tag and nuclear localization signal present in the other sensors. Finally, the *caudal 3'UTR* was inserted in the AscI site downstream of the *d2EGFP-Cad* sequence.

UAS-Bcd constructs

The open reading frame of the five *bicoid* isoforms (GenBank accessions NM_057477, NM_169157, NM_169159, NM_176411, NM_176410) were amplified by PCR from a *Drosophila* embryonic cDNA library using forward primers 5'- CGGGTACCATGGCGCAA CCGCCG-3' (for isoforms A, D and G), 5'- CGGGTACCATGCCCAAGCCAGATGTCTTT CCCTCAG-3' (for isoform E) and 5'-GGCGGCCGGAAAATGCCCAAGCCAGAGGAG-3' (for isoform F), and the reverse primer 5'- GCGGATCCATTGAAGCAGTAGGCAAACTGCG-3'. The reverse primer does not include the stop codon. All isoforms were then fused C-terminally

with the 6xMyc tag, followed by a stop codon, and cloned into the pUASp2 vector, a derivative of pUASp [S8] kindly provided by P. Rorth.

miR-308m construct

We designed a mutant version of the precursor hairpin of *Drosophila miR-308* (miRBase accession MI0000419), called *miR-308m*, carrying compensatory mutations that restore binding to *cadM1*. Additional changes were made to preserve the secondary structure of the precursor (see Figure 3D), which is likely to be important for processing of the microRNA. The miR-308m precursor, 50 nucleotides of flanking genomic sequence and the SV40 3'UTR were synthesized (Mr.Gene) and cloned downstream of tubulin α-1 promoter and H2B-mRFPruby [S9]. The entire construct was cloned into the BamHI site of transformation vector pMi-(3xP3-DsRed-SV40) [S10].

Drosophila stocks and crosses

In vivo sensor lines were generated using ϕC31-mediated integration into the JB38F landing site on chromosome 2 [S4]. Constructs were injected into the *nos-φC31-int;P[attP.w+.attP]JB38F* stock, which expresses the ϕC31 integrase [S11]. *nos-φC31-int* was crossed away and the sensor lines were kept as homozygous stocks.

The UAS-Bcd lines were generated by P-element mediated transformation in a *yw* stock. For each isoform we assayed at least two independent, homozygous viable transgenic lines. Expression of Bcd was driven by the *nanos-GAL4:VP16* driver [S12] and confirmed by immunohistochemical stainings in early blastoderm embryos using an anti-Myc antibody.

The *miR-308m* construct was inserted on the same chromosome as the *cadM1* sensor, by *Minos* mediated transformation.

We crossed flies carrying the relevant sensor and UAS-Bcd constructs to *nanos-GAL4:VP16* [S12] and selected heterozygous females carrying a single copy of each transgene. All measurements were made on embryos laid by these females (crossed to *yw* males). As controls we used embryos laid by females carrying a single copy the relevant sensor and *nanos-GAL4:VP16*.

Quantification of sensor fluorescence

EGFP fluorescence was quantified in live blastoderm embryos at nuclear cycle 11 (the interphase preceding mitosis 11) on a Leica MZ16F fluorescence stereoscope equipped with the GFP3 Ultra filter set, the EL6000 light source and the DFC300FX digital camera. The embryos were dechorionated for 1-2 minutes in 50% bleach, mounted in halocarbon oil and photographed under a 2x objective (230x magnification), focusing on the surface of the blastoderm. Experimental and control samples were measured in parallel to account for daily variations in temperature, lamp intensity etc., under constant microscope and camera settings. Mean fluorescence intensity was quantified within a given rectangular area at the centre of each embryo, using ImageJ, and normalized against that of control embryos taken during the same session. At least 20 embryos were measured per sample and statistical significance was assessed using Student's t-test.

Quantification of sensor mRNA levels

mRNA quantification was carried out on dissected ovaries (10 females per sample) and early embryos (egg collections of less than 2 hours at 25˚C) derived from females of the appropriate genotype. Ovaries and embryos were homogenized in 150 uL TRIzol reagent (Ambion). TRIzol was added to 1 ml and RNA was extracted according to the manufacturer's instructions, with an additional chloroform extraction step prior to RNA precipitation. Extracted RNA was treated with 2 units of TURBO DNase (Ambion) for 20 minutes at 37˚C, followed by a second round of TRIzol extraction. RNA integrity was assessed by agarose gel electrophoresis and on an Agilent 2200 Tapestation.

cDNA was synthesized with the SuperScript III First-Strand Synthesis System for RT-PCR (Invitrogen). In all reactions, 25 ng random hexamers were added to 2.5 µg total RNA. For each sample, we included a control omitting the reverse transcriptase (minus-RT).

Real time PCR reactions were performed in triplicate with iTaq Universal SYBR Green Supermix (Biorad) on a BioRad CFX96 real-time PCR machine. The levels of sensor mRNA were quantified in relation to the *tubulin α1* mRNA; primer sequences 5'-CTCAATATGCGT GAATGTATCTCTATCCATGTTG-3' and 5'-GCTCCAAGCAGTAGAGCTCC-3' for tubulin α1, and 5'-CTCAATATGCGTGAAGGTACCATGG-3' and 5'-CTTGTGGCCGTTTACGTCG-3' for the sensors. Both forward primers span exon-exon boundaries. Minus-RT controls were run in parallel, and melting curve analysis was performed after each PCR to confirm the specificity of amplification. Amplification efficiencies were calculated using a standard curve for each run and each primer pair.

Data were analyzed with the gene expression analysis module of the BioRad CFX Manager software. For each sample, the level of sensor mRNA was normalized against the level of *tubulin α1* mRNA using the delta-delta-Ct method, taking into account the amplification efficiencies determined for each primer pair.

<u>^{32}P-labelled probes for *in vitro* binding studies</u>

Templates for the RNA probes were generated by PCR, using forward primers that carry the T7 promoter sequence (see above). The *BRE(257-319), H1, H2* and *H3* templates were generated using the primers described earlier; the *shSV40* template was generated using primers 5'-GTAATACGACTCACTATAGGGCGAACTAGATCATAATCAGCC-3' and 5'-AGGGGGAGGTGTGGGAGG-3'; the *CU58mer* template was generated using primers 5'-GTAATACGACTCACTATAGGGCGACTCTCTCTCTTCTTCCTCTCTC-3' and 5'- AGAAGA GGAGAGAGAAGGAGAGGAGAAAGAGAGAGAGGAAGAAGAG-3'.

Using these templates, RNA probes were generated by *in vitro* transcription with the MEGAscript T7 kit (Ambion), 5'-end labeled using ^{32}P gamma-labeled ATP and T4 Polynucleotide Kinase (New England Biolabs), and purified on a Sephadex G-50 column. DNA probes containing the Bcd binding site [S3] (*dsDNA* in Figure S3) were generated by annealing primers 5'-GAATTCGCTCTAATCCCCGAA-3' and 5'-GAATTCCGGGGATTAGAGC-3', labeled using ^{32}P alpha-labeled ATP and Klenow polymerase (New England Biolabs), and purification on a Sephadex G-50 column.

<u>Expression and purification of the Bicoid homeodomain</u>

The Bicoid homeodomain was amplified by PCR using primers 5'-GGAATTCCATATGCCACGTCGCACCCGCACC-3' and 5'-CGGGATCCCTACTAGGACTGG TCCTTGTGCTGATC-3' and cloned into the NdeI and BamHI sites of the plasmid pET16b-HisMBPTev (gift from A. Economou; [S13]). pET16b-HisMBPTev carries an N-terminal His-tag, followed by the Maltose Binding protein (MBP), a cleavage site for the TEV protease and the NdeI and BamHI sites for directional cloning. The His-MBP-BcdHD fusion protein was expressed in *E.coli* BL21(DE3)pLys and purified using Protino Ni-TED Resin (Macherey-Nagel). Purity was confirmed on Coomassie-stained SDS-PAGE gels. The Bicoid homeodomain was cleaved from MBP using AcTEV-Protease (Invitrogen); cleavage was confirmed on Coomassie-stained SDS-PAGE gels.

<u>Electrophoretic mobility shift assays</u>

Different amounts of Bicoid homeodomain (0-20 pmole) were incubated with 20-30 fmole ^{32}P-labeled RNA for 10 min on ice, in a 10µl reaction containing 10 mM HEPES pH 7.5, 100 mM KCl, 1 mM MgCl2, 0.5 mM EDTA, 1 mM DTT, 0.5 µg/µl yeast tRNA, 10% glycerol (final concentrations). Prior to binding, the radiolabeled RNAs were heated in the same buffer (without tRNA) at 70°C for 5 min and then chilled on ice for 5 min. The binding reactions were then run on a 12% polyacrylamide gel in 0.5x TBE, at 4°C.

DNA-binding reactions were performed in parallel to confirm functionality of the Bicoid homeodomain (see Figure S3B). The homeodomain was incubated with 2 pmole radiolabeled *dsDNA* probe (see above) for 10 min on ice, in the same conditions used for RNA binding experiments. Radioactive signals was detected on a phosphorimager.

In competition experiments (Figure S3B) the same procedure was followed, but after binding 1µl of unlabeled competitor RNA (at different concentrations) was added to the binding reaction and incubated for an additional 10 min on ice. As with the radiolabeled RNA, the competitor RNAs had been previously incubated at 70°C for 5 min followed by 5 min on ice.

RNA secondary structure and microRNA target predictions

The RNA secondary structure predictions were made using Mfold [S14]. The microRNA target site in *BRE(257-319)* was found using MicroInspector [S15]; it is also found by genome-wide searches for microRNA targets [S16].

Supplemental References

S1. Struhl, G., Struhl, K., and Macdonald, P. M. (1989). The gradient morphogen bicoid is a concentration-dependent transcriptional activator. Cell *57*, 1259–1273.

S2. Ochoa-Espinosa, A., Yu, D., Tsirigos, A., Struffi, P., and Small, S. (2009). Anterior-posterior positional information in the absence of a strong Bicoid gradient. Proc. Natl. Acad. Sci. USA *106*, 3823-3828.

S3. Baird-Titus, J. M., Clark-Baldwin, K., Dave, V., Caperelli, C. A., Ma, J., and Rance, M. (2006). The Solution Structure of the Native K50 Bicoid Homeodomain Bound to the Consensus TAATCC DNA-binding Site. Journal of Molecular Biology *356*, 1137–1151.

S4. Bateman, J. R., Lee, A. M., and Wu, C. T. (2006). Site-specific transformation of Drosophila via phiC31 integrase-mediated cassette exchange. Genetics *173*, 769–777.

S5. Stauber, M., Lemke, S., and Schmidt-Ott, U. (2008). Expression and regulation of caudal in the lower cyclorrhaphan fly Megaselia. Dev. Genes Evol. *218*, 81–87.

S6. Brennecke, J., Hipfner, D. R., Stark, A., Russell, R. B., and Cohen, S. M. (2003). bantam encodes a developmentally regulated microRNA that controls cell proliferation and regulates the proapoptotic gene hid in Drosophila. Cell *113*, 25–36.

S7. Wimmer, E. A., Carleton, A., Harjes, P., Turner, T., and Desplan, C. (2000). Bicoid-independent formation of thoracic segments in Drosophila. Science *287*, 2476–2479.

S8. Rorth, P. (1998). Gal4 in the Drosophila female germline. Mechanisms Of Development *78*, 113–118.

S9. Müller-Taubenberger, A., Vos, M. J., Böttger, A., Lasi, M., Lai, F. P. L., Fischer, M., and Rottner, K. (2006). Monomeric red fluorescent protein variants used for imaging studies in different species. European Journal of Cell Biology *85*, 1119–1129.

S10. Pavlopoulos, A., and Averof, M. (2005). Establishing genetic transformation for comparative developmental studies in the crustacean Parhyale hawaiensis. Proc. Natl. Acad. Sci. U.S.A. *102*, 7888–7893.

S11. Bischof, J., Maeda, R. K., Hediger, M., Karch, F., and Basler, K. (2007). An optimized transgenesis system for Drosophila using germ-line-specific phiC31 integrases. Proc. Natl. Acad. Sci. U.S.A. *104*, 3312–3317.

S12. Van Doren, M., Williamson, A. L., and Lehmann, R. (1998). Regulation of zygotic gene expression in Drosophila primordial germ cells. Current Biology *8*, 243–246.

S13. Gelis, I., Bonvin, A. M. J. J., Keramisanou, D., Koukaki, M., Gouridis, G., Karamanou, S., Economou, A., and Kalodimos, C. G. (2007). Structural basis for signal-sequence recognition by the translocase motor SecA as determined by NMR. Cell *131*, 756–769.

S14. Zuker, M. (2003). Mfold web server for nucleic acid folding and hybridization prediction. Nucleic Acids Research *31*, 3406–3415.

S15. Rusinov, V., Baev, V., Minkov, I. N., and Tabler, M. (2005). MicroInspector: a web tool for detection of miRNA binding sites in an RNA sequence. Nucleic Acids Research *33*, W696–700.

S16. Stark, A., Brennecke, J., Russell, R. B., and Cohen, S. M. (2003). Identification of Drosophila MicroRNA Targets. Plos Biol *1*, e60.